

Time-Averaged Drift Approximations are Inconsistent for Inference in Drift Diffusion Models

Sicheng Liu* Alexander Fengler† Michael J. Frank‡
 Matthew T. Harrison§

Abstract

Drift diffusion models (DDMs) have found widespread use in computational neuroscience and other fields. They model evidence accumulation in simple decision tasks as a stochastic process drifting towards a decision barrier. In models where the drift rate is both time-varying within a trial and variable across trials, the high computational cost for accurate likelihood evaluation has led to the common use of a computationally convenient surrogate for parameter inference, the time-averaged drift approximation (TADA). In each trial, the TADA assumes that the time-varying drift rate can be replaced by its temporal average throughout the trial. This approach enables fast parameter inference using analytical likelihood formulas for DDMs with constant drift. In this work, we show that such an estimator is inconsistent: it does not converge to the true drift, posing a risk of biasing scientific conclusions drawn from parameter estimates produced by TADA and similar surrogates. We provide an elementary proof of this inconsistency in what is perhaps the simplest possible setting: a Brownian motion with piecewise constant drift hitting a one-sided upper boundary. Furthermore, we conduct numerical examples with an attentional DDM (aDDM) to show that the use of TADA systematically misestimates the effect of attention in decision making.

1 Introduction

Drift diffusion models (DDMs) are an important class of models that describe the latent psychological processes underlying simple decision-making scenarios such as two-alternative forced choice experiments [34, 33, 35]. In such

*Division of Applied Mathematics, Brown University. Email: sicheng_liu@brown.edu

†Department of Cognitive and Psychological Sciences, Brown University. Email: alexander_fengler@brown.edu

‡Department of Cognitive and Psychological Sciences, Brown University; Carney Institute for Brain Science, Brown University. Email: michael_frank@brown.edu

§Division of Applied Mathematics, Brown University. Email: matthew_harrison@brown.edu

experiments, a subject must choose between two alternatives, A and B, and the experimenter records both the choice and the time taken to make it. DDMs are used to model the joint distribution over response times and choices and are widely applied in empirical research [30, 4, 22, 28, 20] to extract their interpretable parameters, which can in turn be linked to distinct cognitive and neural mechanisms.

The standard DDM is described by the stochastic differential equation

$$dX(t) = \mu dt + \sigma dW(t) \tag{1}$$

starting at $X(0) = x_0$, where $W(t)$ is a 1D Brownian motion. Decision dynamics are captured by $X(t)$ before the stopping time τ , where

$$\tau \triangleq \inf\{t > 0 : X(t) \notin (\ell, u)\}$$

is the first hitting time of $X(t)$ to the upper boundary u or the lower boundary ℓ , indicating the decision time. The boundary reached at time τ reflects the chosen outcome, which we denote as $C \in \{u, \ell\}$. The parameter vector θ may include $\mu, \sigma, x_0, u, \ell$ or any further parameters that define them. The likelihood function is the **first passage time density (FPTD)** at the boundary C evaluated at τ when viewed as a function of the parameter vector θ . For the standard DDM, the analytic solution for the density and distribution of τ can be mathematically derived in closed form [23, 12, 5, 1], enabling tractable likelihood-based inference for its parameters. As a result, this model has found widespread applications in cognitive neuroscience and mathematical psychology [33, 34, 2, 10, 7, 52, 9].

The standard DDM can be extended in a variety of ways to better capture experimental data and to test hypotheses about the biological mechanisms underlying decision-making. Examples include models with time-varying decision boundaries $u(t)$ and $\ell(t)$ instead of constant thresholds u and ℓ [3, 8, 19, 26, 11], models with more complex stochastic dynamics than Brownian motion [49, 32], and models with trial-by-trial drift rates that covary with exogenous covariates (μ_i or $\mu_i(t)$ for trial i instead of a common drift μ or $\mu(t)$ across trials)[44, 10, 48, 9]. Many of these extensions typically do not admit closed-form expressions for their FPTDs, but numerical methods have been developed to compute the FPTDs of DDMs to facilitate their application, including approaches based on solving Kolmogorov equations [38, 6, 45, 46] and integral equations [39, 40, 27, 29].

When the parameters describing a DDM are both time-varying and trial-varying, for example, when the drift rate is modulated by covariates that vary on a moment-by-moment basis in time, the computational cost of computing different FPTDs on each trial can become too large for practical use. A common approach in this situation is to approximate a time-varying-parameter model with a constant-parameter model that permits fast FPTD evaluation. An open question in the literature is the degree to which these commonly-used approximations lead to valid conclusions about the underlying time-varying models of scientific interest.

In this paper we demonstrate both mathematically and empirically that constant-parameter approximations can lead to substantial statistical biases for parameter inference, suggesting caution for their use. We focus on a class of DDMs called attentional DDMs (aDDMs) and a class of constant-parameter approximations that we call time-averaged drift approximations (TADA). As described in Section 2, aDDMs have time-varying and trial-varying drift rates, and TADA for the aDDM replaces the time-varying drift on each trial with its temporal average over the trial. We focus on these example cases for the following reasons. (i) They are of current practical importance. (ii) Simple versions facilitate exact mathematical analysis of large-sample statistical behavior. (iii) Most existing uses of constant-parameter approximations arise specifically in aDDMs via approaches related to TADA. (iv) In parallel work [16] we develop an efficient method for computing FPTDs in aDDMs, allowing us to numerically compare true and approximate methods for this class of models.

2 Attentional Drift Diffusion Models

A notable class of DDMs that involve trial-varying and time-varying drift rates is the **attentional drift diffusion model (aDDM)** [14]. The aDDM incorporates visual attention as a key factor underlying the decision process behind simple choice behavior. It adjusts the drift rate $\mu(t)$ based on instantaneous attention within a given experimental trial, adopting different values depending on whether the participant fixates on choice options A or B at time t . Specifically, if we let $V(t)$ be the process taking values in $\{A, B\}$ representing the participant’s visual fixation at time t , and let r_A and r_B denote the participant’s numerical ratings of their preferences for options A and B, respectively. The aDDM corresponds to the following SDE (conditioned on V, r_A, r_B) [14],

$$dX(t) = A(V(t), r_A, r_B) dt + \sigma dW(t) \quad (2)$$

where

$$A(v, r_A, r_B) = \begin{cases} \kappa(r_A - \eta r_B) & \text{if } v = A, \\ \kappa(\eta r_A - r_B) & \text{if } v = B, \end{cases}$$

$\eta \in (0, 1)$ is a parameter that reflects the discounting of the non-fixated option, and $\kappa > 0$ parametrizes the overall magnitude of the drift.

In a typical experimental setting, a participant’s fixation trajectory $V(t)$ is captured using an eye-tracker, while the participant’s preference ratings r_A and r_B are collected prior to the choice experiment; together, these are treated as known covariates. Note that $\mu(t) = A(V(t), r_A, r_B)$ is a piecewise constant function which is generally different on each experimental trial, both because a participant’s visual fixation process will generally be different on each trial and because the options presented to the participant can change across trials. As in Eq. (2) we often suppress the dependence on trials in our notation.

The dependence on within-trial covariates, here specifically the fixation times, poses significant computational challenges. The analytical results available for

the standard DDM no longer apply, as the drift term in the aDDM varies over time. Moreover, because fixation trajectories are unique for each trial, computations cannot be shared across trials, necessitating likelihood evaluation on a trial-by-trial basis. As a result, existing numerical methods, such as the Kolmogorov equation methods and integral equation methods, become impractical for the large datasets typically encountered in experimental studies. Parameter inference in the aDDM can take days or even weeks for sizable datasets, severely limiting its applicability despite its strong scientific interest.

3 Time-averaged Drift Approximation

Due to these aforementioned computational challenges, researchers have resorted to computationally efficient approximations of the aDDM for likelihood computation to enable statistical inference. One common approach is to adopt what we call the **time-averaged drift approximation (TADA)**. Broadly speaking, this method aims to simplify the computation by summarizing the fixation process $V(t)$ through the proportion of total gaze time allocated to each option to construct a constant “effective” drift, rather than modeling the full sequence of fixation trajectories. Then, the analytical likelihood formula of a standard DDM with that “effective” drift is used to compute the trial likelihood. This approach simplifies away the computational difficulty associated with within-trial covariates, focusing instead on the overall influence of gaze for each trial, and allows for fast statistical computations in practice.

It is worth noting that implementation details may vary across studies employing TADA, although the basic idea is shared. For instance, the piecewise constant averaging method [17] conjectures that for each sample path, conditioned on its first passage time τ , a DDM with drift function $\mu(t)$ can be viewed as a standard DDM whose drift coefficient is given by

$$\frac{1}{\tau} \int_0^\tau \mu(t) dt, \quad (3)$$

and since the aDDM has a piecewise constant drift function $\mu(t) = A(V(t), r_A, r_B)$, this “effective” drift ends up being

$$\begin{aligned} \frac{1}{\tau} \int_0^\tau A(V(t), r_A, r_B) dt = \\ \frac{\text{time fixated at A}}{\tau} A(A, r_A, r_B) + \frac{\text{time fixated at B}}{\tau} A(B, r_A, r_B), \end{aligned} \quad (4)$$

the temporal average drift in the aDDM weighted by gaze times. The gaze-weighted linear accumulator model (GLAM) [42, 21] applies an additional sigmoid transformation to map the gaze-weighted option values to the “effective” drift rate. GLAM also generalizes the DDM to multiple choice options. Nevertheless, the essential assumption underlying all such variants is that only the gaze proportions matter for inference, a simplification that substantially improves computational tractability.

However, despite its widespread usage, the suitability of using TADA to approximate the aDDM (2) has not been quantitatively investigated. To begin with, regardless of how the “effective” drift is defined, TADA is not a well-specified generative model for first passage times since its “effective” drift (3) depends on the first passage time τ itself. Consequently, the so-called TADA “likelihood” is not a valid likelihood function (see also Figure 1) and its corresponding estimators can only be defined in a formal sense. Nevertheless, it has been argued that the aDDM and its piecewise constant averaging variant are equivalent [17]. More commonly, researchers have used TADA as a computational shortcut to fit and test the aDDM [18, 37, 31, 50, 51, 43, 53, 42, 41, 2], implicitly suggesting that, although their likelihoods may differ for individual sample paths, TADA provides a reasonable approximation to the aDDM at the population level of all trial-level covariates. Under this assumption, the maximum likelihood or Bayesian estimators derived from TADA could remain consistent, making it a useful surrogate model for statistical inference and hypothesis testing.

In this work we show that both statements are technically invalid: TADA and the aDDM have different likelihood function (unsurprisingly), and the TADA “maximum likelihood” estimator is inconsistent, as demonstrated by a concrete counterexample in Section 4.2.

4 Mathematical Analysis

In this section we formally prove that a statistical estimator based on a TADA can be statistically inconsistent, meaning that the estimator converges to the wrong value as the number of trials increases. We illustrate inconsistency in a simple example that permits exact mathematical analysis.

4.1 Preliminaries

Here we first summarize the analytical formulas used in the next subsection:

Theorem 4.1. *Let $X(t) = x_0 + \mu t + \sigma W(t)$, and for $b \neq x_0$, let $\tau_b = \inf\{t \geq 0 : X(t) = b\}$ be the first passage time of $X(t)$ to b , then*

1. *For x satisfying $(x - b)(x_0 - b) > 0$ (x and x_0 are on the same side of b), the non-passage density (NPD), which is defined as the sub-probability density of $X(t)$ when the process has not yet hit b , is given by*

$$\begin{aligned} & \mathbb{P}^{x_0}(X(t) \in dx, \tau_b > t) \\ &= \frac{1}{\sqrt{2\pi\sigma^2 t}} e^{\frac{\mu}{\sigma^2}(x-x_0) - \frac{\mu^2}{2\sigma^2}t} \left(e^{-\frac{(x-x_0)^2}{2\sigma^2 t}} - e^{-\frac{(x+x_0-2b)^2}{2\sigma^2 t}} \right) dx \end{aligned} \quad (5)$$

where \mathbb{P}^{x_0} denotes the probability measure under which the process starts at x_0 .

2. For $t > 0$, the first passage time density (FPTD), which is defined as the density of τ_b , is given by

$$\mathbb{P}^{x_0}(\tau_b \in dt) = \frac{|b - x_0|}{\sqrt{2\pi\sigma^2 t^3}} e^{-\frac{(b-x_0-\mu t)^2}{2\sigma^2 t}} dt \quad (6)$$

When $\mu(b - x_0) > 0$, τ_b is an inverse Gaussian random variable¹ $\text{IG}\left(\frac{b-x_0}{\mu}, \left(\frac{b-x_0}{\sigma}\right)^2\right)$; When $\mu(b - x_0) < 0$, Eq.(6) is a subprobability density as $\mathbb{P}(\tau_b < \infty) = e^{\frac{2(b-x_0)\mu}{\sigma^2}} < 1$.

Formula (6) can be derived via various approaches, for example see page 96 of [13] or Chapter 5.4 of [5]. The classical approach involves using the optional sampling theorem to study the Laplace transform of τ_b by constructing suitable exponential martingales. For completeness we include a self-consistent proof of both (5) and (6) in Appendix A.

4.2 An inconsistent example

Next, we give a simple example to show our two core results:

1. Conditional on the first passage time τ , TADA and the aDDM produce different first passage time densities (FPTDs), so they cannot be viewed as equivalent per sample path. In fact, the TADA ‘‘FPTD’’ function does not integrate to 1 with respect to τ .
2. In this example, as the sample size $n \rightarrow \infty$, the TADA estimator always converges to a value strictly greater than the true drift parameter. Hence, it is statistically inconsistent.

We consider a Brownian motion with piecewise constant drift given by

$$dX(t) = \mu \mathbb{1}_{[0,T]}(t) dt + dW(t) \quad (7)$$

starting at $X(0) = 0$ and a constant upper boundary $u(t) = b$, where $b > 0$ and $T > 0$ are known constants, $\mu \in \mathbb{R}$ is the drift parameter to be inferred, and $\mathbb{1}_{[0,T]}(t)$ denotes the indicator function that takes value 1 if $t \in [0, T]$ and

¹The inverse Gaussian distribution $\text{IG}(m, \lambda)$ is a family of continuous probability distributions, where $m > 0$ is the mean and $\lambda > 0$ is the shape parameter. It is supported on $x \in (0, \infty)$, with probability density function and cumulative distribution function given by

$$f(x; m, \lambda) = \sqrt{\frac{\lambda}{2\pi x^3}} e^{-\frac{\lambda(x-m)^2}{2m^2 x}}$$

$$F(x; m, \lambda) = 1 - \frac{1}{2} \text{Erfc}\left(\sqrt{\frac{\lambda}{2x}}\left(\frac{x}{m} - 1\right)\right) + \frac{1}{2} e^{\frac{2\lambda}{m}} \text{Erfc}\left(\sqrt{\frac{\lambda}{2x}}\left(\frac{x}{m} + 1\right)\right)$$

respectively, where Erfc is the complementary error function defined by $\text{Erfc}(x) = \frac{2}{\sqrt{\pi}} \int_x^\infty e^{-z^2} dz$. Its $m = \infty$ limit is the Lévy distribution, corresponding to the special case $\mu = 0$ in Theorem 4.1, which directly follows from the reflection principle of Brownian motion.

0 otherwise. Let $\tau = \inf\{t > 0 : X(t) = b\}$ be the first passage time of $X(t)$ to level b . This can be viewed as an aDDM with only one boundary and one fixed saccade, or an attentional race model with only one accumulator.

We also define

$$\alpha(\mu, t, T) = \begin{cases} \mu & t \leq T \\ \frac{T}{t}\mu & t > T \end{cases} \quad (8)$$

to represent the average of the drift term until time t . This is the ‘‘effective’’ drift constructed by the piecewise constant averaging method [17], which we adopt as the representative form of TADA in our subsequent analysis.

4.2.1 Non-equivalence of FPTDs

When $\tau \leq T$, τ is distributed according to Eq.(6); when $\tau > T$, we view this process as a DDM with a random initial position x_0 , where its density is specified by the NPD in Eq. (5). To obtain the distribution of τ in this case, we integrate Eq. (6) over the NPD. To be more specific, when $\tau > T$, the FPTD $f_{\text{aDDM}}(\tau; \mu)$ is given by $\int_{-\infty}^b \frac{1}{\sqrt{2\pi T}} e^{\mu x - \frac{\mu^2}{2} T} \left(e^{-\frac{x^2}{2T}} - e^{-\frac{(x-2b)^2}{2T}} \right) \frac{b-x}{\sqrt{2\pi(\tau-T)^3}} e^{-\frac{(b-x)^2}{2(\tau-T)}}$ dx , which simplifies to

$$f_{\text{aDDM}}(\tau; \mu) = \begin{cases} \frac{b}{\sqrt{2\pi\tau^3}} e^{-\frac{(b-\mu\tau)^2}{2\tau}} & \tau \leq T \\ \frac{1}{2\sqrt{2\pi\tau^3}} e^{-\frac{(T\mu-b)^2}{2\tau}} \left[e^{\frac{2b\mu(\tau-T)}{\tau}} (T\mu+b) \operatorname{Erfc} \left((T\mu+b) \sqrt{\frac{\tau-T}{2T\tau}} \right) - (T\mu-b) \operatorname{Erfc} \left((T\mu-b) \sqrt{\frac{\tau-T}{2T\tau}} \right) \right] & \tau > T \end{cases} \quad (9)$$

where $\operatorname{Erfc}(x) = \frac{2}{\sqrt{\pi}} \int_x^\infty e^{-z^2} dz$ is the complementary error function² (see details of this calculation in Appendix D.1). In contrast, the TADA FPTD is

$$f_{\text{TADA}}(\tau; \mu) = \frac{b}{\sqrt{2\pi\tau^3}} e^{-\frac{(b-\alpha(\mu, \tau, T)\tau)^2}{2\tau}} = \begin{cases} \frac{b}{\sqrt{2\pi\tau^3}} e^{-\frac{(b-\mu\tau)^2}{2\tau}} & \tau \leq T \\ \frac{b}{\sqrt{2\pi\tau^3}} e^{-\frac{(b-T\mu)^2}{2\tau}} & \tau > T \end{cases} \quad (10)$$

When $\tau \leq T$, Eq.(9) and Eq.(10) are the same, which corresponds to the case where the participant never switches their visual fixation. To compare Eq.(9) and Eq.(10) when $\tau > T$, we study their integrals w.r.t. τ from T to ∞ . The true probability of hitting after T is given by

$$\begin{aligned} \mathbb{P}(\tau > T) &= 1 - \int_0^T \frac{b}{\sqrt{2\pi t^3}} e^{-\frac{(b-\mu t)^2}{2t}} dt \\ &= \frac{1}{2} \operatorname{Erfc} \left(\frac{T\mu-b}{\sqrt{2T}} \right) - \frac{1}{2} e^{2b\mu} \operatorname{Erfc} \left(\frac{T\mu+b}{\sqrt{2T}} \right) \end{aligned} \quad (11)$$

²We use Erfc throughout this paper for notational consistency. However, it can be equivalently expressed in terms of the error function Erf or the normal CDF Φ .

as Eq.(9) is a valid probability density when viewed as a function of τ . However, integrating Eq.(10) w.r.t. τ over (T, ∞) gives

$$\int_T^\infty \frac{b}{\sqrt{2\pi t^3}} e^{-\frac{(b-T\mu)^2}{2t}} dt = \begin{cases} \frac{b}{T\mu-b} \left(1 - \operatorname{Erfc}\left(\frac{T\mu-b}{\sqrt{2T}}\right)\right) & T\mu \neq b \\ \sqrt{\frac{2}{\pi T}} b & T\mu = b \end{cases} \quad (12)$$

We compare Eq.(11) and Eq.(12) when $T\mu = b$: (11) reduces to $\frac{1}{2} \left(1 - e^{-\frac{2b^2}{T}} \operatorname{Erfc}\left(\sqrt{\frac{2}{T}} b\right)\right)$ which is always $\leq \frac{1}{2}$; In contrast, Eq.(12) gives $\sqrt{\frac{2}{\pi T}} b$, which can be any positive number as b and T vary within $(0, \infty)$. As a result, the aDDM FPTD Eq.(9) and the TADA ‘‘FPTD’’ Eq.(10) are different for $\tau > T$ (see Fig.1 for illustration). Hence, the aDDM and TADA are not equivalent, except in the trivial case with no saccades.

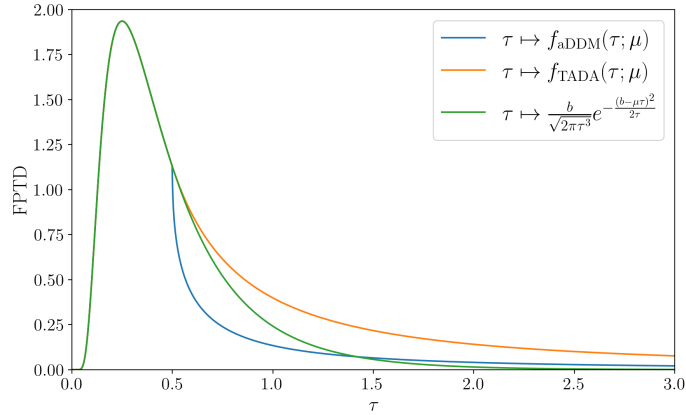


Figure 1: Plots of f_{aDDM} (9) (blue curve), f_{TADA} (10) (orange curve) as functions of τ when $\mu = 2, b = 1, T = 0.5$. The additional green curve is the FPTD when the drift is constant μ instead of $\mu \mathbb{1}_{[0,T]}(t)$. All three functions are the same when $\tau \leq T$, but become different when $\tau > T$. The area under $\tau \mapsto f_{\text{aDDM}}(\tau; \mu)$ and $\tau \mapsto \frac{b}{\sqrt{2\pi\tau^3}} e^{-\frac{(b-\mu\tau)^2}{2\tau}}$ are each 1 while that of $\tau \mapsto f_{\text{TADA}}(\tau; \mu)$ is not 1. This discrepancy arises because the TADA is not a well-specified model, and $f_{\text{TADA}}(\tau; \mu)$ is not a proper probability density function.

4.2.2 Inconsistency of the TADA estimator

In this section, we study the inference of parameter μ using the dataset $(\tau_i)_{i=1}^n$, where τ_1, \dots, τ_n are independent and identically distributed as τ .

We can write the maximum likelihood estimator (MLE)

$$\hat{\mu}_n^{\text{ML}} = \operatorname{argmax}_{\mu} \prod_{i=1}^n f_{\text{aDDM}}(\tau_i; \mu) \quad (13)$$

which maximizes the likelihood in Eq.(9) on dataset $(\tau_i)_{i=1}^n$, and the corresponding TADA “maximum likelihood” estimator

$$\hat{\mu}_n^{\text{TADA}} = \operatorname{argmax}_{\mu} \prod_{i=1}^n f_{\text{TADA}}(\tau_i; \mu) \quad (14)$$

The consistency of $\hat{\mu}_n^{\text{ML}}$ follows from known results about the consistency of MLEs (see Appendix C).

Here we prove that $\hat{\mu}_n^{\text{TADA}}$ is not a consistent estimator of μ . We write the TADA negative log-likelihood

$$\begin{aligned} \ell_n^{\text{TADA}}(\mu \mid \tau_1, \dots, \tau_n) \\ &\triangleq - \sum_{i=1}^n \log f_{\text{TADA}}(\tau_i; \mu) \\ &= -n \log(b) + \frac{n}{2} \log(2\pi) + \sum_{i=1}^n \left(\frac{3}{2} \log \tau_i + \frac{1}{2\tau_i} (b - \alpha(\mu, \tau_i, T)\tau_i)^2 \right) \end{aligned}$$

and $\hat{\mu}_n^{\text{TADA}}$ (14) is given by

$$\hat{\mu}_n^{\text{TADA}} = \operatorname{argmin}_{\mu} \ell_n^{\text{TADA}}(\mu \mid \tau_1, \dots, \tau_n) \quad (15)$$

setting $\frac{\partial \ell_n^{\text{TADA}}}{\partial \mu}$ to 0, we get

$$\begin{aligned} 0 &= \frac{\partial \ell_n^{\text{TADA}}}{\partial \mu}(\hat{\mu}_n^{\text{TADA}} \mid \tau_1, \dots, \tau_n) \\ &= \sum_{i=1}^n \alpha_{\mu}(\hat{\mu}_n^{\text{TADA}}, \tau_i, T) (\alpha(\hat{\mu}_n^{\text{TADA}}, \tau_i, T)\tau_i - b) \end{aligned} \quad (16)$$

where

$$\alpha_{\mu}(\mu, \tau, T) = \frac{\partial}{\partial \mu} \alpha(\mu, \tau, T) = \begin{cases} 1 & t \leq T \\ \frac{T}{t} & t > T \end{cases}$$

One can verify that the second derivative is $\sum_{i=1}^n (\alpha_{\mu}(\hat{\mu}_n^{\text{TADA}}, \tau_i, T))^2 \tau_i > 0$ so $\hat{\mu}_n^{\text{TADA}}$ minimizes ℓ_n^{TADA} . To proceed, we assume that $0 < \tau_1 \leq \dots \leq \tau_m \leq T < \tau_{m+1} \leq \dots \leq \tau_n$, then Eq.(16) becomes

$$\begin{aligned} 0 &= \sum_{i=1}^m (\hat{\mu}_n^{\text{TADA}} \tau_i - b) + \sum_{i=m+1}^n \frac{T}{\tau_i} (T \hat{\mu}_n^{\text{TADA}} - b) \\ &= \left(\sum_{i=1}^m \tau_i \right) \hat{\mu}_n^{\text{TADA}} - mb + \left(\sum_{i=m+1}^n \frac{1}{\tau_i} \right) T^2 \hat{\mu}_n^{\text{TADA}} - \left(\sum_{i=m+1}^n \frac{1}{\tau_i} \right) Tb \end{aligned} \quad (17)$$

which further simplifies to

$$\hat{\mu}_n^{\text{TADA}} = \frac{mb + \left(\sum_{i=m+1}^n \frac{1}{\tau_i} \right) Tb}{\sum_{i=1}^m \tau_i + \left(\sum_{i=m+1}^n \frac{1}{\tau_i} \right) T^2} \quad (18)$$

Dividing both the numerator and denominator of Eq.(18) by n , we can invoke the strong law of large numbers to get

$$\hat{\mu}_n^{\text{TADA}} \xrightarrow{\text{a.s.}} \tilde{\mu}, \text{ where } \tilde{\mu} \triangleq \frac{\mathbb{P}(\tau \leq T)b + \mathbb{E}[\frac{T}{\tau} \mathbb{1}_{\tau > T}]b}{\mathbb{E}[\tau \mathbb{1}_{\tau \leq T}] + \mathbb{E}[\frac{T}{\tau} \mathbb{1}_{\tau > T}]T} \quad (19)$$

Here $\xrightarrow{\text{a.s.}}$ denotes almost sure convergence, which is defined as $\mathbb{P}(\hat{\mu}_n^{\text{TADA}} \rightarrow \tilde{\mu}) = 1$. Since $\mathbb{E}[\tau \mathbb{1}_{\tau \leq T}] < \mathbb{E}[T \mathbb{1}_{\tau \leq T}] = T\mathbb{P}(\tau \leq T)$ and noting that the strict inequality follows from the fact that $\mathbb{P}(\tau < T) > 0$, equation (19) immediately gives $\tilde{\mu} > \frac{b}{T}$. This shows that $\hat{\mu}_n^{\text{TADA}}$ cannot be consistent as the true μ is allowed to be $\leq \frac{b}{T}$. However, we can also prove the following stronger claim:

Theorem 4.2. *For any $\mu \in \mathbb{R}$, we always have $\tilde{\mu} > \max\{\mu, \frac{b}{T}\}$.*

To prove theorem 4.2, we need the following lemmas:

Lemma 4.3. *If $0 < a < A$ and $0 < d < D$, then $\frac{A+d}{a+d} > \frac{A+D}{a+D}$.*

The proof of lemma 4.3 is straightforward.

Lemma 4.4. $\varphi(x) \triangleq xe^{x^2} \text{Erfc}(x)$ is strictly increasing on \mathbb{R} .

Proof of Lemma 4.4. $\varphi'(x) = e^{x^2}(2x^2 + 1) \text{Erfc}(x) - \frac{2}{\sqrt{\pi}}x$. By the bounds on Mill's ratio $e^{x^2} \text{Erfc}(x) > \frac{2}{\sqrt{\pi}} \frac{1}{x + \sqrt{x^2 + 2}}$ (see [25] 7.8.2), we have

$$\varphi'(x) > \frac{2}{\sqrt{\pi}} \frac{2x^2 + 1}{x + \sqrt{x^2 + 2}} - \frac{2}{\sqrt{\pi}}x = \frac{2}{\sqrt{\pi}} \frac{x^2 + 1 - x\sqrt{x^2 + 2}}{x + \sqrt{x^2 + 2}}$$

This is obviously > 0 when $x \leq 0$. When $x > 0$ we can continue to write

$$\begin{aligned} \varphi'(x) &> \frac{2}{\sqrt{\pi}} \frac{(x^2 + 1)^2 - (x\sqrt{x^2 + 2})^2}{(x + \sqrt{x^2 + 2})(x^2 + 1 + x\sqrt{x^2 + 2})} \\ &= \frac{2}{\sqrt{\pi}} \frac{1}{(x + \sqrt{x^2 + 2})(x^2 + 1 + x\sqrt{x^2 + 2})} > 0 \end{aligned}$$

So $\varphi(x)$ is strictly increasing on \mathbb{R} . ■

Proof of Theorem 4.2. Notice that $\mathbb{E}[\frac{T}{\tau} \mathbb{1}_{\tau > T}] < \mathbb{E}[\mathbb{1}_{\tau > T}] = \mathbb{P}(\tau > T)$ so by lemma 4.3 we have

$$\begin{aligned} \tilde{\mu} &= \frac{b}{T} \frac{\mathbb{P}(\tau \leq T)T + \mathbb{E}[\frac{T}{\tau} \mathbb{1}_{\tau > T}]T}{\mathbb{E}[\tau \mathbb{1}_{\tau \leq T}] + \mathbb{E}[\frac{T}{\tau} \mathbb{1}_{\tau > T}]T} \\ &> \frac{b}{T} \frac{\mathbb{P}(\tau \leq T)T + \mathbb{P}(\tau > T)T}{\mathbb{E}[\tau \mathbb{1}_{\tau \leq T}] + \mathbb{P}(\tau > T)T} \\ &= \frac{b}{\mathbb{E}[\tau \mathbb{1}_{\tau \leq T}] + \mathbb{P}(\tau > T)T} \end{aligned}$$

$\mathbb{P}(\tau > T)$ is given by Eq.(11). We can also compute that

$$\begin{aligned} \mathbb{E}[\tau \mathbb{1}_{\tau \leq T}] &= \int_0^T \frac{bt}{\sqrt{2\pi t^3}} e^{-\frac{(b-\mu t)^2}{2t}} dt \\ &= \frac{b}{\mu} \left(1 - \frac{1}{2} \operatorname{Erfc} \left(\frac{T\mu - b}{\sqrt{2T}} \right) - \frac{1}{2} e^{2b\mu} \operatorname{Erfc} \left(\frac{T\mu + b}{\sqrt{2T}} \right) \right) \end{aligned} \quad (20)$$

(see details of this derivation in Appendix D.2). So to prove that $\tilde{\mu} > \mu$, it suffices to prove

$$\frac{b}{\mu \left(1 - \frac{1}{2} \operatorname{Erfc} \left(\frac{T\mu - b}{\sqrt{2T}} \right) - \frac{1}{2} e^{2b\mu} \operatorname{Erfc} \left(\frac{T\mu + b}{\sqrt{2T}} \right) \right) + T \left(\frac{1}{2} \operatorname{Erfc} \left(\frac{T\mu - b}{\sqrt{2T}} \right) - \frac{1}{2} e^{2b\mu} \operatorname{Erfc} \left(\frac{T\mu + b}{\sqrt{2T}} \right) \right)} > \mu$$

which further simplifies to

$$(T\mu + b)e^{2b\mu} \operatorname{Erfc} \left(\frac{T\mu + b}{\sqrt{2T}} \right) > (T\mu - b) \operatorname{Erfc} \left(\frac{T\mu - b}{\sqrt{2T}} \right). \quad (21)$$

Note that this can be rewritten as $\varphi \left(\frac{T\mu + b}{\sqrt{2T}} \right) > \varphi \left(\frac{T\mu - b}{\sqrt{2T}} \right)$ where $\varphi(x) = xe^{x^2} \operatorname{Erfc}(x)$, so by Lemma 4.4, the inequality (21) holds. \blacksquare

5 Numerical Examples

In this section we provide some numerical examples to further demonstrate the inconsistency of $\hat{\mu}_n^{\text{TADA}}$.

5.1 DDM with One-sided Boundary

We first conduct a numerical illustration of our proposed counterexample (7) in Section 4.2. We simulate an i.i.d. dataset of first passage times $(\tau_i)_{i=1}^n$ using Euler-Maruyama discretization of (7) with a sufficiently small time step. With $b = 1$ and $T = 0.5$, we aim to infer μ from the dataset $(\tau_i)_{i=1}^n$.

We compute both the TADA “maximum likelihood” estimator $\hat{\mu}_n^{\text{TADA}}$ (14) and the generic maximum likelihood estimator $\hat{\mu}_n^{\text{ML}}$ (13). We then compare them with the true μ and $\tilde{\mu}$ (19), the derived theoretical large-sample limit of $\hat{\mu}_n^{\text{TADA}}$ ³. The results are summarized in Table 1.

μ	$\hat{\mu}_n^{\text{ML}}$	$\tilde{\mu}$	$\hat{\mu}_n^{\text{TADA}}$
1	0.996	2.613	2.606

Table 1: Values of the true μ , the maximum likelihood estimator $\hat{\mu}_n^{\text{ML}}$ (13), the TADA “maximum likelihood” estimator $\hat{\mu}_n^{\text{TADA}}$ (14) and its limit $\tilde{\mu}$ (19).

The results demonstrate that $\hat{\mu}_n^{\text{TADA}}$ converges to $\tilde{\mu}$ rather than the true μ as $n \rightarrow \infty$, confirming its inconsistency. In contrast, the maximum likelihood estimator $\hat{\mu}_n^{\text{ML}}$ correctly converges to μ .

³ $\mathbb{P}(\tau \leq T)$ and $\mathbb{E}[\tau \mathbb{1}_{\tau \leq T}]$ are given by Eq.(11) and Eq.(20) respectively. $\mathbb{E}[\frac{T}{\tau} \mathbb{1}_{\tau > T}]$ can be calculated with numerical integration accurately.

5.2 DDM with Double-sided Boundaries

In this section we conduct a parameter recovery study for a DDM with one upper boundary and one lower boundary. The model is defined as

$$dX(t) = A(V(t)) dt + \sigma dW(t),$$

$$\text{where } A(v) \triangleq \begin{cases} \mu_1 & \text{if } v = \text{A}, \\ \mu_2 & \text{if } v = \text{B}. \end{cases} \quad (22)$$

The drift function $\mu(t) = A(V(t))$ is a piecewise constant function alternating between μ_1 and μ_2 depending on the fixation trajectory $V(t)$. For each trial i , the fixation trajectory $V_i(t)$ was sampled from a gamma process to mimic the switching of attention in psychological experiments. Compared to the previous example in Section 5.1, this model includes two absorbing boundaries and incorporates an attentional drift mechanism more closely aligned with the aDDM (2), while remaining a simplified variant that excludes option-value covariates.

We simulate a collection of $n = 10,000$ visual fixation trajectories $(V_i)_{i=1}^n$ and the corresponding dataset $((\tau_i, C_i))_{i=1}^n$ from a prescribed DDM model (22) with alternating drifts μ_1, μ_2 , constant diffusion $\sigma = 1$ and symmetric constant boundaries $u = -\ell = 1.5$ starting at $x_0 = -0.2$. The average number of fixations per trial in our simulation was 3.806.

The TADA follows the same approach as in the one-boundary case: for each trial it replaces the time-varying drift rate $\mu(t)$ of the DDM with the constant drift rate $\tau^{-1} \int_0^\tau \mu(t) dt$. This constant drift is further used to evaluate the formulas for first passage time densities on the upper and lower boundaries of a standard DDM (1) with two boundaries, which are available as infinite series [23, 12, 5]. This allows us to compute the estimator $\hat{\mu}_{1,n}^{\text{TADA}}$ and $\hat{\mu}_{2,n}^{\text{TADA}}$ from the simulated data. The computations of the generic MLEs $\hat{\mu}_{1,n}^{\text{ML}}$ and $\hat{\mu}_{2,n}^{\text{ML}}$, are however more involved, as the first passage time density of the DDM (22) is analytically intractable. In our parallel work [16], we develop an algorithm for the fast and accurate computation of first passage time densities in DDMs with “multi-stage” structures, such as those with piecewise constant drift functions like (22) and (2). We use this algorithm to evaluate the likelihood and obtain the MLEs. The estimation results are summarized in Table 2.

μ_1	$\hat{\mu}_{1,n}^{\text{ML}}$	$\hat{\mu}_{1,n}^{\text{TADA}}$	μ_2	$\hat{\mu}_{2,n}^{\text{ML}}$	$\hat{\mu}_{2,n}^{\text{TADA}}$
1	1.003	1.684	-0.8	-0.796	-1.478

Table 2: Values of the true μ_1, μ_2 , the maximum likelihood estimators $\hat{\mu}_{1,n}^{\text{ML}}, \hat{\mu}_{2,n}^{\text{ML}}$, the TADA “maximum likelihood” estimators $\hat{\mu}_{1,n}^{\text{TADA}}, \hat{\mu}_{2,n}^{\text{TADA}}$.

From the table, we conclude again that $\hat{\mu}_{1,n}^{\text{ML}}$ and $\hat{\mu}_{2,n}^{\text{ML}}$ accurately estimate the true values of μ_1 and μ_2 respectively, while $\hat{\mu}_{1,n}^{\text{TADA}}$ and $\hat{\mu}_{2,n}^{\text{TADA}}$ do not. Similarly to the results in Example 5.1, $\hat{\mu}_{1,n}^{\text{TADA}}$ and $\hat{\mu}_{2,n}^{\text{TADA}}$ overestimates the amplitude

of the drifts. However, the theoretical large sample limits of $\hat{\mu}_{1,n}^{\text{TADA}}$ and $\hat{\mu}_{2,n}^{\text{TADA}}$ are unknown in this case.

5.3 Attentional DDM

We conclude this section by studying the consequences of using TADA to perform statistical inference of the parameters in an aDDM (2).

Similar to the setup in Example 5.2, we simulate $n = 10,000$ visual fixation trajectories $(V_i(t))_{i=1}^n$ from a gamma process. The corresponding option ratings $((r_{A,i}, r_{B,i}))_{i=1}^n$ are drawn from a discrete uniform distribution over $\{1, 2, 3, 4, 5\}$, and the associated decision data $((\tau_i, C_i))_{i=1}^n$ are generated accordingly. In this example, we set the boundaries to be symmetric ($u = -\ell$) and aim to estimate all four free parameters from data, namely η, κ, u and x_0 . The likelihood is then evaluated using both the TADA (as described in Section 3) and the methods proposed in [16], from which the corresponding maximum likelihood estimators are obtained.

The true parameters are set to $\kappa = 0.5, u = 2$, and $x_0 = 0.5$. Since η is the primary parameter of interest for testing the aDDM, we vary its true value from 0 to 1 in increments of 0.05 to examine the estimation error across different levels of η . The relations of the true η , the TADA “maximum likelihood” estimator $\hat{\eta}_n^{\text{TADA}}$, and the MLE $\hat{\eta}_n^{\text{ML}}$ are shown in Figure 2.

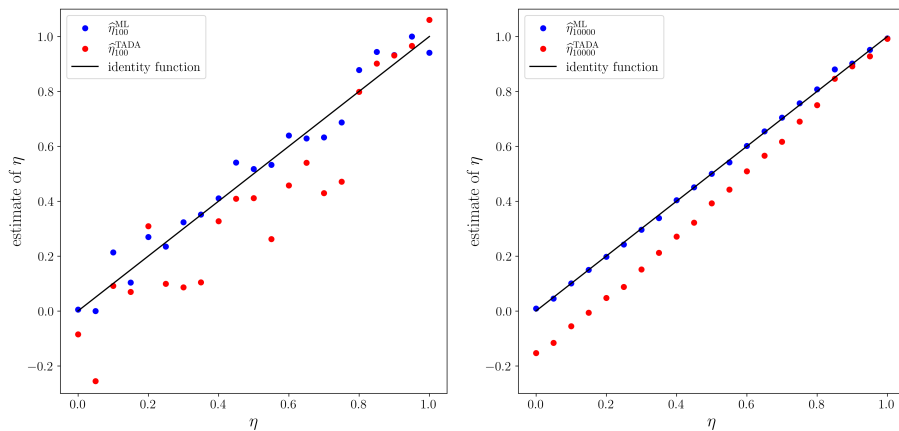


Figure 2: Plots of the values of estimator $\hat{\eta}_n^{\text{TADA}}$ (red points) and $\hat{\eta}_n^{\text{ML}}$ (blue points) against the true value η with $n = 100$ (left subplot) and $n = 10,000$ (right subplot). The black line is the plot of the identity function $y = x$ which serves as the reference for consistent estimation. $\eta = 0$ means maximal attentional effect that the decision-maker completely ignore the non-fixated item in evidence accumulating, whereas $\eta = 1$ corresponds to no attentional effect, in which case the model reduces to the standard DDM.

From Figure 2, we can see that the $\hat{\eta}_n^{\text{ML}}$ aligns closely with the identity line $y = x$, even for small sample size ($n = 100$), and becomes nearly exact when

$n = 10,000$. This indicates the consistency of $\hat{\eta}_n^{\text{ML}}$: as the sample size grows, the estimator converges to the true parameter. However, $\hat{\eta}_n^{\text{TADA}}$ systematically underestimates η . Even when $n = 10,000$, the red points remain well below the identity line, showing persistent asymptotic bias that does not vanish with larger n . This confirms that the TADA “maximum likelihood” estimator is inconsistent. It is worth noting that $\eta = 1$ corresponds to the case with no attentional effect, where the model reduces to the standard DDM. In this case, the TADA “likelihood” coincide with the analytical likelihood solution of the standard DDM, and the bias therefore vanishes. As η decreases toward 0 (indicating stronger attentional effects), the bias $\hat{\eta}_n^{\text{TADA}} - \eta$ grows larger. Indeed, the original aDDM study [14], which fitted the model via expensive forward simulation, reported a maximum-likelihood estimate of 0.3, a value in the range where TADA exhibits substantial bias. When η is close to 0 (approximately < 0.2), $\hat{\eta}_n^{\text{TADA}}$ even takes negative values, which are not physically meaningful. Indeed, a recent study comparing TADA fits to multiple datasets across humans and monkeys often reported individuals with $\eta < 0$ [18].

We note that, in this specific example, if researchers are primarily interested in qualitative conclusions of the aDDM rather than quantitative parameter estimation, the use of TADA may still yield meaningful insights. Scientifically, Figure 2 shows that, at least in this specific example, while TADA underestimates the magnitude of the attentional parameter η , it nonetheless preserves the monotonic relationship between the estimated and true values. This means that TADA still captures the direction and relative strength of attentional effects: trials with stronger true attentional modulation (smaller η) still produce smaller estimated values, although this monotonic relationship may only become evident with a large dataset (e.g., $n = 10,000$). However, we caution that this monotonicity relationship is specific to the present simulation and may attenuate or even fail under different task structures, model variants, or parameter regimes, so even the qualitative conclusions based on TADA may not hold in other settings.

6 Conclusion

In this paper, we present several simple yet compelling examples demonstrating that “maximum likelihood” estimators based on the TADA approximation yield inconsistent estimates of the drift parameters. We establish this inconsistency through theoretical derivations for the DDM with a single absorbing boundary, support it with numerical simulations, and further demonstrate it numerically for the DDM with two absorbing boundaries, as well as for the full aDDM.

We note that although this work focuses on the canonical multiplicative form of the aDDM, our main conclusion regarding estimator inconsistency extends to other model variants as well, as long as they also admit a TADA type estimator described in Section 3. Examples include models incorporating additive gaze biases, where fixations add to rather than scale the evidence for attended options, and multi-attribute attention models, where fixations modulate attention

to individual attributes rather than entire options.

Numerous recent studies on the aDDM have relied on the TADA or similar approximations that ignore the fixation trajectory [18, 37, 31, 50, 51, 43, 53, 42, 41, 2]. This paper suggests that such an approach may not be as reliable as previously assumed, owing to the demonstrated inconsistency of the resulting estimators. On the other hand, employing TADA for downstream scientific analyses does not necessarily lead to incorrect conclusions. However, since TADA is based on an intuitive approximation rather than a rigorous statistical foundation, there is no theoretical guarantee that its results are reliable across settings, and we hence consider our findings as a note of caution in that regard.

Our findings underscore the need for a fast and statistically sound algorithm for computing the likelihood function of the aDDM, either exactly or through mathematically justified approximations. Our parallel work [16] introduces such a fast and accurate algorithm for evaluating first-passage time densities for DDMs, achieving state-of-the-art inference speed and beating previous methods by orders of magnitude for aDDMs. In fact, this work enabled the efficient execution of the numerical experiments presented in this paper. We recommend that researchers adopt the methods in [16] and corresponding software for aDDM data analysis and develop further extensions of that framework to handle more general classes of DDMs, as its correctness is grounded in rigorous mathematical theory while offering computational efficiency comparable to TADA.

Acknowledgements

This work was supported by the National Institute of Mental Health (grants P50 MH119467-01 and P50 MH106435-06A1), the Office of Naval Research (MURI Award N00014-23-1-2792), and the Brainstorm Program at the Robert J. and Nancy D. Carney Institute for Brain Science. S.L. was additionally supported by the JBB Endowed Graduate Fellowship in Brain Science.

References

- [1] Steven P Blurton, Miriam Kesselmeier, and Matthias Gondan. Fast and accurate calculations for cumulative first-passage time distributions in wiener diffusion models. *Journal of Mathematical Psychology*, 56(6):470–475, 2012.
- [2] James F Cavanagh, Thomas V Wiecki, Angad Kochar, and Michael J Frank. Eye tracking and pupillometry are indicators of dissociable latent decision processes. *Journal of Experimental Psychology: General*, 143(4):1476, 2014.
- [3] Paul Cisek, Geneviève Aude Puskas, and Stephany El-Murr. Decisions in changing conditions: the urgency-gating model. *Journal of Neuroscience*, 29(37):11560–11571, 2009.
- [4] J. Clithero. Response times in economics: Looking through the lens of sequential sampling models. *CSN: General Cognitive Neuroscience (Topic)*, 2016.
- [5] David Roxbee Cox. *The theory of stochastic processes*. Routledge, 2017.
- [6] Adele Diederich and Jerome R Busemeyer. Simple matrix methods for analyzing diffusion models of choice probability, choice response time, and simple response time. *Journal of Mathematical Psychology*, 47(3):304–322, 2003.
- [7] Takahiro Doi, Yunshu Fan, Joshua I Gold, and Long Ding. The caudate nucleus contributes causally to decisions that balance reward and uncertain visual information. *ELife*, 9:e56694, 2020.
- [8] Jan Drugowitsch, Rubén Moreno-Bote, Anne K. Churchland, Michael N. Shadlen, and Alexandre Pouget. The cost of accumulating evidence in perceptual decision making. *The Journal of Neuroscience*, 32(11):3612–3628, March 2012.
- [9] Alexander Fengler, Krishn Bera, Mads L Pedersen, and Michael J Frank. Beyond drift diffusion models: Fitting a broad class of decision and reinforcement learning models with hddm. *Journal of Cognitive Neuroscience*, 34(10):1780–1805, 2022.
- [10] Michael J Frank, Chris Gagne, Erika Nyhus, Sean Masters, Thomas V Wiecki, James F Cavanagh, and David Badre. fmri and eeg predictors of dynamic decision parameters during human reinforcement learning. *Journal of Neuroscience*, 35(2):485–494, 2015.
- [11] Nadja Ging-Jehli, James F. Cavanagh, Minkyu Ahn, David J. Segar, Wael F. Asaad, and Michael J. Frank. Basal ganglia components have distinct computational roles in decision-making dynamics under conflict and uncertainty. *PLOS Biology*, 23(1):e3002978, 2025.

- [12] Matthias Gondan, Steven P Blurton, and Miriam Kesselmeier. Even faster and even more accurate first-passage time densities and distributions for the wiener diffusion model. *Journal of Mathematical Psychology*, 60:20–22, 2014.
- [13] Ioannis Karatzas and Steven Shreve. *Brownian motion and stochastic calculus*, volume 113. Springer Science & Business Media, 1991.
- [14] Ian Krajbich, Carrie Armel, and Antonio Rangel. Visual fixations and the computation and comparison of value in simple choice. *Nature neuroscience*, 13(10):1292–1298, 2010.
- [15] Erich L Lehmann and George Casella. *Theory of point estimation*. Springer Science & Business Media, 2006.
- [16] Sicheng Liu, Alexander Fengler, Michael J Frank, and Matthew T Harrison. Efficient inference in first passage time models. *arXiv preprint arXiv:2503.18381*, 2025.
- [17] Gaia Lombardi and Todd Hare. Piecewise constant averaging methods allow for fast and accurate hierarchical bayesian estimation of drift diffusion models with time-varying evidence accumulation rates, Oct 2021.
- [18] Shira M Lupkin and Vincent B McGinty. Monkeys exhibit human-like gaze biases in economic decisions. *Elife*, 12:e78205, 2023.
- [19] Gaurav Malhotra, David S Leslie, Casimir JH Ludwig, and Rafal Bogacz. Time-varying decision boundaries: insights from optimality analysis. *Psychonomic bulletin & review*, 25(3):971–996, 2018.
- [20] Milica Milosavljevic, Jonathan Malmaud, Alexander Huth, Christof Koch, and Antonio Rangel. The drift diffusion model can account for value-based choice response times under high and low time pressurethe drift diffusion model can account for value-based choice response times under high and low time pressure. *Judgment and Decision Making*, 5(6):437–449, 2010.
- [21] Felix Molter, Armin W Thomas, Hauke R Heekeren, and Peter NC Mohr. Glambox: A python toolbox for investigating the association between gaze allocation and decision behaviour. *PloS one*, 14(12):e0226428, 2019.
- [22] C. Myers, A. Interian, and A. Moustafa. A practical introduction to using the drift diffusion model of decision-making in cognitive psychology, neuroscience, and health sciences. *Frontiers in Psychology*, 13, 2022.
- [23] Daniel J Navarro and Ian G Fuss. Fast and accurate calculations for first-passage times in wiener diffusion models. *Journal of mathematical psychology*, 53(4):222–230, 2009.
- [24] Bernt Øksendal and Bernt Øksendal. *Stochastic differential equations*. Springer, 2003.

- [25] Frank W Olver, Daniel W Lozier, Ronald F Boisvert, and Charles W Clark. *NIST handbook of mathematical functions*. Cambridge university press, 2010.
- [26] James J Palestro, Emily Weichart, Per B Sederberg, and Brandon M Turner. Some task demands induce collapsing bounds: Evidence from a behavioral analysis. *Psychonomic bulletin & review*, 25(4):1225–1248, 2018.
- [27] Liam Paninski, Adrian Haith, and Gabor Szirtes. Integral equation methods for computing likelihoods and their derivatives in the stochastic integrate-and-fire model. *Journal of Computational Neuroscience*, 24:69–79, 2008.
- [28] Mads L. Pedersen, M. Frank, and G. Biele. The drift diffusion model as the choice rule in reinforcement learning. *Psychonomic Bulletin & Review*, 24:1234–1251, 2017.
- [29] Goran Peskir. On integral equations arising in the first-passage problem for brownian motion. *Journal of Integral Equations and Applications*, 14(4):397–423, 2002.
- [30] J. Peters and M. D’Esposito. The drift diffusion model as the choice rule in inter-temporal and risky choice: A case study in medial orbitofrontal cortex lesion patients and controls. *PLoS Computational Biology*, 16, 2019.
- [31] Jorge Ramírez-Ruiz and Rubén Moreno-Bote. Optimal allocation of finite sampling capacity in accumulator models of multialternative decision making. *Cognitive Science*, 46(5):e13143, 2022.
- [32] Amir Hosein Hadian Rasanan, Jamal Amani Rad, and David K Sewell. Are there jumps in evidence accumulation, and what, if anything, do they reflect psychologically? an analysis of lévy flights models of decision-making. *Psychonomic Bulletin & Review*, 31(1):32–48, 2024.
- [33] Roger Ratcliff. A theory of memory retrieval. *Psychological review*, 85(2):59, 1978.
- [34] Roger Ratcliff and Gail McKoon. The diffusion decision model: theory and data for two-choice decision tasks. *Neural computation*, 20(4):873–922, 2008.
- [35] Roger Ratcliff, Philip L. Smith, Scott D. Brown, and Gail McKoon. Diffusion decision model: Current issues and history. *Trends in Cognitive Sciences*, 20(4):260–281, 2016.
- [36] Adrien Saumard and Jon A Wellner. Log-concavity and strong log-concavity: a review. *Statistics surveys*, 8:45, 2014.
- [37] Pradyumna Sepulveda, Marius Usher, Ned Davies, Amy A Benson, Pietro Ortoleva, and Benedetto De Martino. Visual attention modulates the integration of goal-relevant evidence and not value. *elife*, 9:e60705, 2020.

- [38] Maxwell Shinn, Norman H Lam, and John D Murray. A flexible framework for simulating and fitting generalized drift-diffusion models. *ELife*, 9:e56938, 2020.
- [39] Philip L Smith. Stochastic dynamic models of response time and accuracy: A foundational primer. *Journal of mathematical psychology*, 44(3):408–463, 2000.
- [40] Philip L Smith and Roger Ratcliff. Modeling evidence accumulation decision processes using integral equations: Urgency-gating and collapsing boundaries. *Psychological review*, 129(2):235, 2022.
- [41] Armin W Thomas, Felix Molter, and Ian Krajbich. Uncovering the computational mechanisms underlying many-alternative choice. *Elife*, 10:e57012, 2021.
- [42] Armin W Thomas, Felix Molter, Ian Krajbich, Hauke R Heekeren, and Peter NC Mohr. Gaze bias differences capture individual choice behaviour. *Nature human behaviour*, 3(6):625–635, 2019.
- [43] Chih-Chung Ting and Sebastian Gluth. Unraveling information processes of decision-making with eye-tracking data. *Frontiers in Behavioral Economics*, 3:1384713, 2024.
- [44] Brandon M. Turner, Leendert van Maanen, and B. Forstmann. Informing cognitive abstractions through neuroimaging: the neural drift diffusion model. *Psychological review*, 122 2:312–336, 2015.
- [45] Andreas Voss and Jochen Voss. Fast-dm: A free program for efficient diffusion model analysis. *Behavior research methods*, 39(4):767–775, 2007.
- [46] Andreas Voss and Jochen Voss. A fast numerical algorithm for the estimation of diffusion model parameters. *Journal of Mathematical Psychology*, 52(1):1–9, 2008.
- [47] E Weinan, Tiejun Li, and Eric Vanden-Eijnden. *Applied stochastic analysis*, volume 199. American Mathematical Soc., 2021.
- [48] Thomas V Wiecki, Imri Sofer, and Michael J Frank. Hddm: Hierarchical bayesian estimation of the drift-diffusion model in python. *Frontiers in neuroinformatics*, 7:14, 2013.
- [49] Eva Marie Wieschen, Andreas Voss, and Stefan Radev. Jumping to conclusion? a lévy flight model of decision making. *TQMP*, 16(2):120–132, 2020.
- [50] Xiaozhi Yang and Ian Krajbich. A dynamic computational model of gaze and choice in multi-attribute decisions. *Psychological Review*, 130(1):52, 2023.

- [51] Xiaozhi Yang, Chris Retzler, Ian Krajbich, Roger Ratcliff, and Marios G Philiastides. Attention to brand labels affects, and is affected by, evaluations of product attractiveness. *Frontiers in Behavioral Economics*, 2:1274815, 2024.
- [52] Michael M Yartsev, Timothy D Hanks, Alice Misun Yoon, and Carlos D Brody. Causal contribution and dynamical encoding in the striatum during evidence accumulation. *Elife*, 7:e34929, 2018.
- [53] Veronika Zilker. Attentional dynamics of evidence accumulation explain why more numerate people make better decisions under risk. *Scientific Reports*, 14(1):18788, 2024.

A Proof of Theorem 4.1

Here we present a self-consistent derivation of both (5) and (6) using Kolmogorov forward equations. The connections of diffusion processes and partial differential equations (PDEs) are well-established results in stochastic analysis and can be found in standard references, such as [13, 24, 47]. This approach has the advantage of being easily generalizable to more complex diffusion processes and two-sided boundaries.

Proof of Theorem 4.1.1. Without loss of generality we assume $b > x_0$ (i.e. $x = b$ is the upper boundary). Denote the NPD under \mathbb{P}^{x_0} by $u(x, t)$ where $x < b$. It satisfies the following initial-boundary value problem of the Kolmogorov forward equation⁴ (see the Chapter 8 of [47]):

$$\begin{aligned} u_t &= -\mu u_x + \frac{1}{2}\sigma^2 u_{xx} & \text{for } t > 0, x \in (-\infty, b) \\ u(x, 0) &= \delta(x - x_0) & \text{for } x \in (-\infty, b) \\ u(b, t) &= 0 & \text{for } t > 0 \end{aligned} \quad (23)$$

where $\delta(\cdot)$ is the Dirac delta measure at 0. To solve (23), let

$$u(x, t) = e^{\frac{\mu}{\sigma^2}(x-x_0) - \frac{\mu^2}{2\sigma^2}t} v(x - x_0, t),$$

and v is the Green's function that satisfies

$$\begin{aligned} v_t &= \frac{1}{2}\sigma^2 v_{yy} & \text{for } t > 0, y \in (-\infty, b - x_0) \\ v(y, 0) &= \delta(y) & \text{for } y \in (-\infty, b - x_0) \\ v(b - x_0, t) &= 0 & \text{for } t > 0 \end{aligned}$$

By method of images, we get

$$v(y, t) = \frac{1}{\sqrt{2\pi\sigma^2 t}} \left(e^{-\frac{y^2}{2\sigma^2 t}} - e^{-\frac{(y-2(b-x_0))^2}{2\sigma^2 t}} \right)$$

Correspondingly,

$$u(x, t) = \frac{1}{\sqrt{2\pi\sigma^2 t}} e^{\frac{\mu}{\sigma^2}(x-x_0) - \frac{\mu^2}{2\sigma^2}t} \left(e^{-\frac{(x-x_0)^2}{2\sigma^2 t}} - e^{-\frac{(x+x_0-2b)^2}{2\sigma^2 t}} \right) \quad (24)$$

for $x < b$. ■

Proof of Theorem 4.1.2. Here we prove the case where $b > x_0$ and $\mu \geq 0$. Denote the density of τ_b under \mathbb{P}^{x_0} as $f_{\tau_b}(t)$, by definition

$$f_{\tau_b}(t) = -\frac{d}{dt} \mathbb{P}^{x_0}(\tau_b > t)$$

⁴Also known as Fokker-Planck equation in physics.

$\mathbb{P}^{x_0}(\tau_b > t) = \int_{-\infty}^b u(x, t) dx$ represents the net probability flow rate through $x = b$ (see the Chapter 8 of [47]). We can further use the PDE (23) to continue to write

$$\begin{aligned}
f_{\tau_b}(t) &= -\frac{d}{dt} \int_{-\infty}^b u(x, t) dx \\
&= -\int_{-\infty}^b u_t(x, t) dx \\
&= -\int_{-\infty}^b \left(-\mu u_x(x, t) + \frac{1}{2}\sigma^2 u_{xx}(x, t) \right) dx \\
&= \mu \int_{-\infty}^b u_x(x, t) dx - \frac{1}{2}\sigma^2 \int_{-\infty}^b u_{xx}(x, t) dx \\
&= \mu(u(b, t) - u(-\infty, t)) - \frac{1}{2}\sigma^2(u_x(b, t) - u_x(-\infty, t)) \\
&= -\frac{1}{2}\sigma^2 u_x(b, t)
\end{aligned}$$

u is given by (24), from which we can compute

$$f_{\tau_b}(t) = \frac{b - x_0}{\sqrt{2\pi\sigma^2 t^3}} e^{-\frac{(b-x_0-\mu t)^2}{2\sigma^2 t}}$$

■

B Log-concavity of the Likelihood (9)

In this section we prove that the likelihood function (9) is a strict log-concave function of μ . It suffices to show that $\frac{\partial^2}{\partial \mu^2} \log f_{\text{aDDM}}(\tau; \mu) < 0$.

When $\tau \leq T$, we have $\frac{\partial^2}{\partial \mu^2} \log f_{\text{aDDM}}(\tau; \mu) = -\tau < 0$; When $\tau > T$, we write

$$\begin{aligned}
f_{\text{aDDM}}(\tau; \mu) &= \int_{-\infty}^b \frac{1}{\sqrt{2\pi T}} e^{\mu x - \frac{\mu^2}{2} T} \left(e^{-\frac{x^2}{2T}} - e^{-\frac{(x-2b)^2}{2T}} \right) \frac{b-x}{\sqrt{2\pi(\tau-T)^3}} e^{-\frac{(b-x)^2}{2(\tau-T)}} dx \\
&\triangleq \frac{e^{-\frac{\mu^2}{2} T}}{2\pi\sqrt{T(\tau-T)^3}} \int_{-\infty}^b e^{\mu x} g(x) dx
\end{aligned}$$

where

$$g(x) \triangleq (b-x) \left(e^{-\frac{x^2}{2T}} - e^{-\frac{(x-2b)^2}{2T}} \right) e^{-\frac{(b-x)^2}{2(\tau-T)}}$$

is independent of μ . When μ is in any compact sub-interval in \mathbb{R} , $|xe^{\mu x}g(x)|$ and $|x^2e^{\mu x}g(x)|$ can be easily dominated by L^1 functions, hence by Lebesgue's dominated convergence theorem we have

$$\begin{aligned}
\frac{\partial}{\partial \mu} \int_{-\infty}^b e^{\mu x} g(x) dx &= \int_{-\infty}^b x e^{\mu x} g(x) dx \\
\frac{\partial^2}{\partial \mu^2} \int_{-\infty}^b e^{\mu x} g(x) dx &= \int_{-\infty}^b x^2 e^{\mu x} g(x) dx
\end{aligned}$$

and consequently,

$$\frac{\partial^2}{\partial \mu^2} \log f_{\text{aDDM}}(\tau; \mu) = -T + \frac{\int_{-\infty}^b x^2 e^{\mu x} g(x) dx}{\int_{-\infty}^b e^{\mu x} g(x) dx} - \left(\frac{\int_{-\infty}^b x e^{\mu x} g(x) dx}{\int_{-\infty}^b e^{\mu x} g(x) dx} \right)^2 \quad (25)$$

Define the exponential tilting of g as

$$h_\mu(x) = \frac{e^{\mu x} g(x)}{\int_{-\infty}^b e^{\mu x} g(x) dx}$$

$h_\mu(x)$ is a probability density function on $(-\infty, b)$. Let Y_μ be a random variable with density $h_\mu(x)$, then we can interpret Eq.(25) as

$$\frac{\partial^2}{\partial \mu^2} \log f_{\text{aDDM}}(\tau; \mu) = -T + \text{Var}[Y_\mu] \quad (26)$$

Let $V(x) = -\log h_\mu(x)$ so that $h_\mu(x) = e^{-V(x)}$, we can compute that

$$V''(x) = \frac{1}{T} + \frac{1}{\tau - T} + \frac{1}{(x - b)^2} + \left(\frac{2b}{T}\right)^2 \frac{e^{\frac{2b}{T}(x-b)}}{(1 - e^{\frac{2b}{T}(x-b)})^2} > \frac{1}{T} + \frac{1}{\tau - T}$$

i.e., V is $\frac{1}{T} + \frac{1}{\tau - T}$ -strongly convex. By Poincaré's inequality for strictly log-concave measures (see, for example Proposition 10.1 of [36]) we have

$$\text{Var}[Y_\mu] \leq \frac{1}{\frac{1}{T} + \frac{1}{\tau - T}} = \frac{\tau - T}{\tau} T < T$$

Hence from Eq.(26) we have $\frac{\partial^2}{\partial \mu^2} \log f_{\text{aDDM}}(\tau; \mu) < 0$ for $\tau > T$. ■

C Regularity Conditions for the Consistency of $\hat{\mu}_n^{\text{ML}}$

When τ_1, \dots, τ_n are independent and identically distributed as τ , we can show the consistency of $\hat{\mu}_n^{\text{ML}} = \hat{\mu}_n^{\text{ML}}(\tau_1, \dots, \tau_n)$.

First, we write the likelihood equation

$$\frac{\partial}{\partial \mu} \ell_n^{\text{aDDM}}(\mu \mid \tau_1, \dots, \tau_n) = 0 \quad (27)$$

where $\ell_n^{\text{aDDM}}(\mu \mid \tau_1, \dots, \tau_n) \triangleq -\sum_{i=1}^n \log f_{\text{aDDM}}(\tau_i; \mu)$ is the negative log-likelihood function. We prove that Eq.(27) has a root $\hat{\mu}_n = \hat{\mu}_n(\tau_1, \dots, \tau_n)$ that converges to the true value μ_0 in probability by verifying the following regularity conditions (see theorem 6.3.7 of [15]):

- **Identifiability:** We aim to show that $f_{\text{aDDM}}(\tau; \mu_1) = f_{\text{aDDM}}(\tau; \mu_2)$ for all $\tau > 0$ implies $\mu_1 = \mu_2$. Considering when $\tau \leq T$, $f_{\text{aDDM}}(\tau; \mu_1) = f_{\text{aDDM}}(\tau; \mu_2)$ immediately leads to

$$(b - \mu_1\tau)^2 = (b - \mu_2\tau)^2$$

holds for any $0 < \tau \leq T$, so either $\mu_1 = \mu_2$ or $(\mu_1 + \mu_2)\tau = 2b$ for $0 < \tau \leq T$. The latter case implies $\mu_1 + \mu_2 = b/\tau = 0$, which contradicts the fact that b is positive, so μ_1 must equal μ_2 . When $\tau > T$, $\mu_1 = \mu_2$ automatically gives $f_{\text{aDDM}}(\tau; \mu_1) = f_{\text{aDDM}}(\tau; \mu_2)$. Hence, we conclude that $\mu_1 = \mu_2$.

- **Common support:** We claim that for any $\mu \in \mathbb{R}$, $f_{\text{aDDM}}(\tau; \mu)$ has common support $\tau \in (0, \infty)$. When $0 < \tau \leq T$ this is obvious; when $\tau > T$, lemma 4.4 implies $\varphi\left((T\mu + b)\sqrt{\frac{\tau - T}{2T\tau}}\right) > \varphi\left((T\mu - b)\sqrt{\frac{\tau - T}{2T\tau}}\right)$ where $\varphi(x) \triangleq xe^{x^2} \text{Erfc}(x)$. This inequality establishes the positivity of $f_{\text{aDDM}}(\tau; \mu)$.
- The true μ lies in the interior of the parameter space \mathbb{R} as \mathbb{R} is an open set.
- For a.e. τ , $f_{\text{aDDM}}(\tau; \mu)$ is differentiable w.r.t. μ .

so $\hat{\mu}_n$ converges in probability to the true μ as $n \rightarrow \infty$.

In Appendix B we have proven that $\log f_{\text{aDDM}}(\tau; \mu)$ is a strictly concave function of μ , so $\hat{\mu}_n$ is in fact the maximum likelihood estimator $\hat{\mu}_n^{\text{ML}}$. So $\hat{\mu}_n^{\text{ML}}$ is consistent.

D Supplemental Derivations

D.1 Derivation of Eq.(9)

When $\tau > T$, we have

$$\begin{aligned} & f_{\text{aDDM}}(\tau; \mu) \\ &= \int_{-\infty}^b \frac{1}{\sqrt{2\pi T}} e^{\mu x - \frac{\mu^2}{2}T} \left(e^{-\frac{x^2}{2T}} - e^{-\frac{(x-2b)^2}{2T}} \right) \frac{b-x}{\sqrt{2\pi(\tau-T)^3}} e^{-\frac{(b-x)^2}{2(\tau-T)}} dx \\ &\triangleq I_1 - I_2 \end{aligned}$$

where

$$\begin{aligned} I_1 &\triangleq \int_{-\infty}^b \frac{1}{\sqrt{2\pi T}} e^{\mu x - \frac{\mu^2}{2}T} e^{-\frac{x^2}{2T}} \frac{b-x}{\sqrt{2\pi(\tau-T)^3}} e^{-\frac{(b-x)^2}{2(\tau-T)}} dx \\ I_2 &\triangleq \int_{-\infty}^b \frac{1}{\sqrt{2\pi T}} e^{\mu x - \frac{\mu^2}{2}T} e^{-\frac{(x-2b)^2}{2T}} \frac{b-x}{\sqrt{2\pi(\tau-T)^3}} e^{-\frac{(b-x)^2}{2(\tau-T)}} dx \end{aligned}$$

We can compute

$$\begin{aligned}
I_1 &= \int_{-\infty}^b \frac{1}{\sqrt{2\pi T}} \frac{b-x}{\sqrt{2\pi(\tau-T)^3}} e^{\mu x - \frac{\mu^2}{2} T - \frac{x^2}{2T} - \frac{(b-x)^2}{2(\tau-T)}} dx \\
&\quad \text{(Complete the square)} \\
&= \int_{-\infty}^b \frac{1}{\sqrt{2\pi T}} \frac{b-x}{\sqrt{2\pi(\tau-T)^3}} e^{-\frac{(T\mu-b)^2}{2\tau}} e^{-\frac{\tau}{2T(\tau-T)}(x-T\mu-\frac{Tb}{\tau}+\frac{T^2\mu}{\tau})^2} dx \\
&\quad \text{(Let } M_1 = \frac{\tau-T}{\tau}(T\mu-b), N = \frac{\tau-T}{\tau}\text{)} \\
&= \frac{e^{-\frac{(T\mu-b)^2}{2\tau}}}{2\pi\sqrt{T(\tau-T)^3}} \int_{-\infty}^b (b-x) e^{-\frac{(x-M_1-b)^2}{2TN}} dx \\
&\quad \text{(Let } y = -x + M_1 + b\text{)} \\
&= \frac{e^{-\frac{(T\mu-b)^2}{2\tau}}}{2\pi\sqrt{T(\tau-T)^3}} \int_{M_1}^{\infty} (y-M_1) e^{-\frac{y^2}{2TN}} dy \\
&= \frac{e^{-\frac{(T\mu-b)^2}{2\tau}}}{2\pi\sqrt{T(\tau-T)^3}} \left(\int_{M_1}^{\infty} y e^{-\frac{y^2}{2TN}} dy - M_1 \int_{M_1}^{\infty} e^{-\frac{y^2}{2TN}} dy \right) \\
&= \frac{e^{-\frac{(T\mu-b)^2}{2\tau}}}{2\pi\sqrt{T(\tau-T)^3}} \left(TN e^{-\frac{M_1^2}{2TN}} - M_1 \sqrt{\frac{\pi TN}{2}} \operatorname{Erfc}\left(\frac{M_1}{\sqrt{2TN}}\right) \right) \\
&\quad \text{(Substitute } M_1, N, \text{ and simplify)} \\
&= \frac{T e^{-\frac{(T\mu-b)^2}{2T}}}{2\pi\tau\sqrt{T(\tau-T)}} - \frac{e^{-\frac{(T\mu-b)^2}{2\tau}}}{2\sqrt{2\pi\tau^3}} (T\mu-b) \operatorname{Erfc}\left((T\mu-b)\sqrt{\frac{\tau-T}{2T\tau}}\right)
\end{aligned}$$

and similarly

$$\begin{aligned}
I_2 &= \int_{-\infty}^b \frac{1}{\sqrt{2\pi T}} \frac{b-x}{\sqrt{2\pi(\tau-T)^3}} e^{\mu x - \frac{\mu^2}{2} T - \frac{(x-2b)^2}{2T} - \frac{(b-x)^2}{2(\tau-T)}} dx \\
&\quad \text{(Complete the square)} \\
&= \int_{-\infty}^b \frac{1}{\sqrt{2\pi T}} \frac{b-x}{\sqrt{2\pi(\tau-T)^3}} e^{-\frac{(T\mu+b)^2}{2\tau} + 2\mu b} e^{-\frac{\tau}{2T(\tau-T)}(x-T\mu+\frac{Tb}{\tau}+\frac{T^2\mu}{\tau}-2b)^2} dx \\
&\quad \text{(Let } M_2 = \frac{\tau-T}{\tau}(T\mu+b), N = \frac{\tau-T}{\tau}\text{)} \\
&= \frac{e^{-\frac{(T\mu+b)^2}{2\tau} + 2\mu b}}{2\pi\sqrt{T(\tau-T)^3}} \int_{-\infty}^b (b-x) e^{-\frac{(x-M_2-b)^2}{2TN}} dx \\
&\quad \text{(Let } y = -x + M_2 + b\text{)} \\
&= \frac{e^{-\frac{(T\mu+b)^2}{2\tau} + 2\mu b}}{2\pi\sqrt{T(\tau-T)^3}} \int_{M_2}^{\infty} (y-M_2) e^{-\frac{y^2}{2TN}} dy \\
&= \frac{e^{-\frac{(T\mu+b)^2}{2\tau} + 2\mu b}}{2\pi\sqrt{T(\tau-T)^3}} \left(\int_{M_2}^{\infty} y e^{-\frac{y^2}{2TN}} dy - M_2 \int_{M_2}^{\infty} e^{-\frac{y^2}{2TN}} dy \right) \\
&= \frac{e^{-\frac{(T\mu+b)^2}{2\tau} + 2\mu b}}{2\pi\sqrt{T(\tau-T)^3}} \left(TN e^{-\frac{M_2^2}{2TN}} - M_2 \sqrt{\frac{\pi TN}{2}} \operatorname{Erfc}\left(\frac{M_2}{\sqrt{2TN}}\right) \right) \\
&\quad \text{(Substitute } M_2, N, \text{ and simplify)}
\end{aligned}$$

$$= \frac{T e^{-\frac{(T\mu-b)^2}{2T}}}{2\pi\tau\sqrt{T(\tau-T)}} - \frac{e^{-\frac{(T\mu+b)^2}{2\tau} + 2\mu b}}{2\sqrt{2\pi\tau^3}} (T\mu + b) \operatorname{Erfc}\left((T\mu + b)\sqrt{\frac{\tau-T}{2T\tau}}\right)$$

Subtract I_2 from I_1 yields the desired result in (9). ■

D.2 Derivation of Eq.(20)

$$\begin{aligned} \mathbb{E}[\tau \mathbb{1}_{\tau \leq T}] &= \int_0^T \frac{b}{\sqrt{2\pi t}} e^{-\frac{(\mu t - b)^2}{2t}} dt \\ &= \frac{b}{\sqrt{2\pi\mu}} \int_0^T \left(\frac{\mu t + b}{2t^{3/2}} + \frac{\mu t - b}{2t^{3/2}} \right) e^{-\frac{(\mu t - b)^2}{2t}} dt \\ &= \frac{b}{\sqrt{2\pi\mu}} \left(\int_0^T \frac{\mu t + b}{2t^{3/2}} e^{-\frac{(\mu t - b)^2}{2t}} dt + e^{2b\mu} \int_0^T \frac{\mu t - b}{2t^{3/2}} e^{-\frac{(\mu t + b)^2}{2t}} dt \right) \\ &\quad (\text{Let } y = \frac{\mu t - b}{\sqrt{t}}, z = \frac{\mu t + b}{\sqrt{t}}, \text{ then } dy = \frac{\mu t + b}{2t^{3/2}} dt, dz = \frac{\mu t - b}{2t^{3/2}} dt) \\ &= \frac{b}{\sqrt{2\pi\mu}} \left(\int_{-\infty}^{\frac{T\mu - b}{\sqrt{T}}} e^{-\frac{y^2}{2}} dy + e^{2b\mu} \int_{\infty}^{\frac{T\mu + b}{\sqrt{T}}} e^{-\frac{z^2}{2}} dz \right) \\ &= \frac{b}{\mu} \left(1 - \frac{1}{2} \operatorname{Erfc}\left(\frac{T\mu - b}{\sqrt{2T}}\right) - \frac{1}{2} e^{2b\mu} \operatorname{Erfc}\left(\frac{T\mu + b}{\sqrt{2T}}\right) \right) \end{aligned}$$
■